



1           **Locally Produced Sedimentary Biomarkers in High-Altitude Catchments Outweigh**

2                           **Upstream River Transport in Sedimentary Archives**

3    Alex Brittingham<sup>1,2</sup>, Michael T. Hren<sup>3</sup>, Samuel Spitzschuch<sup>1</sup>, Phil Glauberman<sup>4,5,6</sup>, Yonaton  
4    Goldsmith<sup>2</sup>, Boris Gasparyan<sup>5</sup> and Ariel Malinsky-Buller<sup>7</sup>

5

6    1: Department of Anthropology, University of Connecticut, Storrs, Connecticut, USA

7    2: The Fredy & Nadine Herrmann Institute of Earth Sciences, The Hebrew University of

8    Jerusalem, Jerusalem, Israel

9    3: Department of Earth Sciences, University of Connecticut, Storrs, Connecticut, USA

10   4: The Catalan Institute of Human Paleoecology and Social Evolution (IPHES) and Universitat

11   Rovirai I Virgili, Tarragona, Spain

12   5: Institute of Archaeology and Ethnography, National Academy of Sciences of the Republic of

13   Armenia, Yerevan, Armenia

14   6: Department of Early Prehistory and Quaternary Ecology, University of Tübingen, Tübingen,

15   Germany

16   7: The Institute of Archaeology, The Hebrew University of Jerusalem, Jerusalem, Israel

17   *Correspondence to:* Alex Brittingham, alexander.brittingham@mail.huji.ac.il



18 **Abstract:** Sedimentary records of lipid biomarkers such as leaf wax *n*-alkanes are not only  
19 influenced by ecosystem turnover and physiological changes in plants, they are also influenced by  
20 earth surface processes integrating these signals. The integration of biomarkers into the  
21 sedimentary record and the effects of integration processes on recorded environmental signals are  
22 complex and not fully understood. To determine the depositional constraints on biomarker records  
23 in a high-altitude small catchment system, we collected both soil and stream sediments along a  
24 1000 m altitude transect (1500 – 2500 masl) in the Areguni Mountains, a subrange of the Lesser  
25 Caucasus Mountains in Armenia. We utilize the existence of a treeline at ~ 2000 masl, which  
26 separates alpine meadow above from deciduous forest below, to assess the relative contribution of  
27 upstream biomarker transport to local vegetation input in the stream. We find that average chain  
28 length (ACL), hydrogen isotope ( $\delta D$ ) and carbon isotope ( $\delta^{13}C$ ) values of *n*-alkanes are  
29 significantly different in soils collected above and below the treeline. However, samples collected  
30 from the stream sediments do not integrate these signals quantitatively. As the stream drops below  
31 the treeline, the ACL,  $\delta D$  and  $\delta^{13}C$  values of *n*-alkanes preserved in streambed sediments reflect a  
32 bias toward *n*-alkanes sourced from trees. This suggests that there is either 1) minimal  
33 transportation of organic matter from the more open vegetation in higher elevations, or 2) greater  
34 production of target biomarkers by trees and shrubs found at lower elevations results in  
35 overprinting of stream signals by local vegetation. Though this latter observation may preclude  
36 using *n*-alkanes to measure past treeline movement in these mountains,  $\delta D$  values of biomarkers  
37 in fluvial deposits in these settings are more likely to record local hydrological changes rather than  
38 changes in upstream fractionation differences associated with vegetation turnover.

39



## 40 1. Introduction

41 Mountain regions are important hubs for biodiversity and can provide refuge for a number  
42 of endemic species of flora and fauna (Antonelli et al., 2018). However, these high-altitude  
43 environments are often particularly vulnerable to climate change (Guisan and Theurillat, 2000).  
44 Therefore, gaining an understanding of sensitivity of these regions to past climate change is  
45 important for projecting the effects of future climate change on fragile ecosystems. The so called  
46 Caucasus Region in particular has been identified as a biodiversity hotspot covering the Republics  
47 of Armenia, Georgia, Azerbaijan, and parts of the Russian Federation, Türkiye, and Iran, supports  
48 a wide variety of plant and animal species (Zazanashvili, 2009; Gasparyan and Glauberman, 2022).  
49 To better understand climate and environmental change in both the past and the present, it is  
50 necessary to refine our understanding and interpretation of paleoclimate records in this region.  
51 Specifically, we are interested in understanding the sedimentary processes involved in the  
52 formation, transport, recycling, and accumulation of organic biomarkers in sedimentary archives  
53 and assessing whether these archives record a local environmental signal or are a mix of local and  
54 transported organic material.

55 Normal alkanes (*n*-alkanes) are an important component of the epicuticular wax in  
56 terrestrial plants. This waxy coating on plants protects against ultraviolet damage, water loss and  
57 predation (Jetter et al., 2006). Specific compounds in this wax, such as *n*-alkanes, are a useful tool  
58 for reconstructing past environmental changes through the analysis of the distribution of alkane  
59 homologues as well as their stable hydrogen ( $\delta D$ ) and carbon ( $\delta^{13}C$ ) isotope values. Previous  
60 research in the Greater and Lesser Caucasus Mountains has documented the applicability of the  
61 average chain length (ACL) of leaf wax biomarkers as a tool for differentiating between grassy



62 and deciduous vegetation (Bliedtner et al., 2018; Trigui et al., 2019), though on a global scale ACL  
63 does not differentiate well between vegetation types (Bush and McInerney, 2013).

64 The biggest driver of the carbon isotope ( $\delta^{13}\text{C}$ ) values of plant tissue is the photosynthetic  
65 pathway of the plant (Diefendorf and Freimuth, 2017).  $\text{C}_3$  plants, which thrive in areas with cooler  
66 growing season temperatures, have more negative  $\delta^{13}\text{C}$  values than do  $\text{C}_4$  plants, which thrive in  
67 warmer growing season temperatures (Ehleringer et al., 1977).  $\text{C}_3$  vegetation is further influenced  
68 by water use efficiency, as water stress influences the  $c_i/c_a$  ratio of plants (Farquhar et al., 1982).  
69  $\delta^{13}\text{C}$  values in lipids generally follow the same trends, and  $\text{C}_3$  plants have more negative  $\delta^{13}\text{C}$  lipid  
70 values than  $\text{C}_4$  plants (Diefendorf and Freimuth, 2017). However, carbon fractionation of lipids is  
71 not consistent in different classes of plants (Pedentchouk et al., 2008; Sikes et al., 2013; Diefendorf  
72 et al., 2011).

73 The hydrogen isotope ( $\delta\text{D}$ ) values of *n*-alkanes in terrestrial plants record the  $\delta\text{D}$  values of  
74 environmental water (Sachse et al., 2012). This is typically reflective of  $\delta\text{D}$  values in precipitation,  
75 though precipitation  $\delta\text{D}$  values can also undergo positive shifts due to soil evaporation. The  $\delta\text{D}$   
76 values of plant waxes are also influenced by fractionation during biological synthesis of lipids,  
77 which imparts a strong negative fractionation on  $\delta\text{D}$  values, as well as transpiration of leaf water  
78 (Gamarra et al., 2016). The fractionation between meteoric water and lipids is typically larger in  
79 gymnosperms than in angiosperms (Pedentchouk et al., 2008; Oakes and Hren, 2016).

80 Despite the benefits in measuring  $\delta\text{D}$  and  $\delta^{13}\text{C}$  values in *n*-alkanes for understanding  
81 environmental and hydrological processes, not all the processes modifying isotope values from  
82 plant to *n*-alkane deposition are well understood. Sedimentary integration is one of the most poorly  
83 understood aspects of this process (Sachse et al., 2012). A number of studies on the integration of  
84 leaf waxes in catchments have been published in recent years which help clarify these processes



85 (Alewell et al., 2016; Feakins et al., 2018a; Häggi et al., 2016a; Hemingway et al., 2016; Ponton  
86 et al., 2014; Suh et al., 2019). However, most of these studies have focused on large river systems  
87 rather than first order streams. Thus, the sedimentary processes involved in the formation,  
88 transport, recycling, and accumulation of organic biomarkers in first and second order streams are  
89 not well understood. One challenge in assessing these processes in small streams is that the  
90 environment and plant communities are often homogenous, and thus it is not possible to  
91 differentiate between local and upstream transported organic material. To better understand  
92 transport processes affecting organic material in small catchments, we studied a set of streams in  
93 the Dany River, a tributary of the Barepat River, located in the Areguni Mountains in the Lesser  
94 Caucasus Range. This stream system is divided into two distinct ecological regions by the treeline  
95 (at ~ 2000 masl), which separates alpine meadow above the tree line (2000 – 2500 masl) from  
96 deciduous forest below (1500 – 2000 masl). To evaluate the input of *n*-alkanes from upstream  
97 transported organic material relative to vegetation near the stream, we collected soil samples on  
98 the slopes of the mountains from both above- and below the treeline throughout the watershed and  
99 sediments deposited in the streambed along an elevation transect. Comparing the hillslope  
100 sedimentary biomarkers and the streambed sedimentary biomarkers allows assessment of the input  
101 of *n*-alkanes locally produced by vegetation compared to those transported in stream sediments  
102 within the catchment.

103 An additional motivation of this research is that treelines are a vulnerable feature of higher  
104 altitude environments. Previous research in the Areguni Mountains study area has assessed the  
105 relationship between treeline dynamics and climate forcing in the past (Ghukasyan et al., 2010;  
106 Montoya et al., 2013; Malinsky-Buller et al., 2021; Tornero et al., 2016), and the Pleistocene  
107 sediments uncovered at archaeological sites at Kalavan village within this area have the potential



108 to reconstruct this relationship. However, in order to reconstruct these systems in the past it is  
109 important to understand modern biomarkers integration processes in the first and second order  
110 streams and their potential effects on the sedimentary archives of the Areguni Mountains.

## 111 **2. Methods**

### 112 **2.1 Sample Collection and Extraction**

113 Hillslope soil samples were collected in September 2018 along an altitude transect (1500 – 2500  
114 masl) above the Dany River watershed, a first order tributary of the Barepat River in the Areguni  
115 Mountains, Armenia (Fig 1), which traverses the treeline at ~2000 masl. Soil samples were  
116 collected by first clearing the top ~10 cm of soil to remove roots. Stream bed sediment samples  
117 were collected from the Dany River throughout the altitude transect at intervals of ~100 m in  
118 altitude. In all cases, roughly 100 g of sediment were collected for extraction of *n*-alkanes. In order  
119 to extract *n*-alkanes, samples were extracted using a Soxhlet apparatus with 2:1  
120 dichloromethane:methanol for 48 hours. Following lipid extraction, *n*-alkanes were separated with  
121 silica gel column chromatography and quantified on a Thermo-Scientific Trace GC Ultra  
122 (Manufacturer) fitted with a split–splitless (SSL) injector and flame ionization detector (FID) using  
123 a BP-5 column (30 m × 0.25 mm i.d., 0.25 μm film thickness) with He as the carrier (1.5 ml/min).  
124 Odd over even predominance (OEP) (Eq. 1) and average chain length (ACL) (Eq. 2) were used to  
125 evaluate distributions of *n*-alkanes (REF). We also calculated  $P_{aq}$ , an *n*-alkane proxy to evaluate  
126 the possible biomarker contribution of aquatic and emergent plants (Eq. 3) (Ficken et al., 2000).

$$127 \text{ OEP} = \frac{C_{25} + C_{27} + C_{29} + C_{31} + C_{33}}{C_{24} + C_{26} + C_{28} + C_{30} + C_{32}}$$

$$128 \text{ ACL} = \frac{25 * C_{25} + 27 * C_{27} + 29 * C_{29} + 31 * C_{31} + 33 * C_{33}}{C_{25} + C_{27} + C_{29} + C_{31} + C_{33}}$$



129 
$$Paq = \frac{C_{23} + C_{25}}{C_{23} + C_{25} + C_{29} + C_{31}}$$

130 **2.3 Stable Isotope Analysis**

131  $\delta D$  and  $\delta^{13}C$  values of individual *n*-alkanes were measured with a Thermo GC-Isolink coupled  
132 with a Thermo Scientific MAT 253 (manufacturer) isotope ratio mass spectrometer with a BP-5  
133 column (30 m  $\times$  0.25 mm i.d., 0.25  $\mu m$  film thickness). Oven temperature was set at 50°C for 1  
134 min, ramped to 180°C at 12°C/min, then ramped to 320°C at 6°C/min and held for 4 min. Internal  
135 standards (Mix A5 from A. Schimmelman) were run every four samples across a range of  
136 concentrations to correct for size effects. Standard deviations were 0.5‰ for  $\delta^{13}C$  and 4‰ for  $\delta D$ .  
137 Isotope ratios (R) were converted to  $\delta X$  ( $\delta^{13}C$  and  $\delta D$ ) values (Eq. 3) and are expressed in permill  
138 (‰).

139 
$$\delta X = \left( \frac{R_{\text{Sample}}}{R_{\text{Standard}}} - 1 \right) * 1000$$

140

141 **3. Results**

142 **3.1. Alkane abundances**

143 The most abundant alkane homolog in samples collected in the Areguni Mountains is the  
144  $C_{29}$  or  $C_{31}$  alkane, which is typical for terrestrial plants. Odd numbered alkanes are significantly  
145 more abundant than even numbered alkanes, and the OEP of all samples averages 11.2, with a  
146 range from 7.4-18.4. There is no significant difference between the mean OEP of soil (11.1) and  
147 stream (11.3) samples in the watershed. These values are similar to those previously measured in  
148 the Greater and Lesser Caucasus Mountains (Trigui et al., 2019; Bliedtner et al., 2018).



149           The mean average chain length (ACL) of all samples averages 29.7, with a range from 28.4  
150 to 31.8 (Fig 3). In soils above the treeline, the average ACL value is 30.6 (range of 29.8-31.8). In  
151 soils below the treeline, the average ACL value is 29.5 (range of 28.4-30.4). There is a significant  
152 difference between the average ACL values of the above treeline and below treeline soils  
153 ( $p < 0.001$ ). Stream sediment above the treeline has an average ACL value of 29.7 (range of 29.1-  
154 30.2) and stream sediments below the treeline have an average ACL value of 29.3 (range of 28.6  
155 to 30.0). The stream sediments from below the treeline have a significantly ( $p < 0.001$ ) lower  
156 average ACL value than those above the treeline.

157           The  $P_{aq}$  values of *n*-alkanes in these samples suggests a mostly terrestrial origin of the  
158 organic matter. Higher  $P_{aq}$  values indicate contributions of floating and emergent macrophytes.  
159 However, we do not find a significant difference between the  $P_{aq}$  values in the stream sediments  
160 when compared to the soil samples, indicating that the organic load of the stream sediments is  
161 mostly of terrestrial origin. Terrestrial plants have average  $P_{aq}$  values of 0.09, with emergent plants  
162 averaging 0.25 (Ficken et al., 2000). Only eight of the 51 samples in this study had  $P_{aq}$  values above  
163 0.20, four stream and four soil samples. This indicates that there was not a significant contribution  
164 of aquatic plants in the Dany stream sediments, and the biomarker load is primarily terrestrial in  
165 origin.

### 166 **3.2. $\delta D$ and $\delta^{13}C$ values**

167           The  $\delta^{13}C$  values in soils and stream sediments collected from the Areguni Mountains reflect  
168 a  $C_3$  landscape, which is typical in Armenia.  $\delta^{13}C$  values in all samples ranged from -36.0 to -  
169 32.3‰ (Fig 4). The range is similar for both soil samples (-35.9 to -32.3‰) and stream samples (-  
170 36.0 to -32.5‰). However, there is a significant difference in the  $\delta^{13}C$  values of above and below  
171 treeline samples, both in the stream and soil samples collected. Above the treeline,  $\delta^{13}C$  values in



172 soils averages -34.9‰, and below the treeline soil alkanes average -33.3‰. Stream sediment  $\delta^{13}\text{C}$   
173 values average -35.0‰ above the treeline and -33.6‰ below the treeline. In both cases, these  
174 values are significant ( $p < 0.0001$ , student's t-test).  $\Delta^{13}\text{C}$  values in stream samples exhibit a step-  
175 like behavior, with ~2‰ shift to more negative values as the stream drops below the treeline.

176 The  $\delta\text{D}$  values measured in soil samples collected in the catchment ranged from -144 to -  
177 185‰ (Fig 5). These values were significantly ( $p < 0.001$ , student's t-test). More negative in above  
178 treeline sediments (-175‰) than in below treeline sediments (-156‰). This is also true in sediment  
179 collected from stream samples, which are significantly more negative above the treeline (-175‰)  
180 than below the treeline (-158‰). As with the  $\delta^{13}\text{C}$  values, the  $\delta\text{D}$  values of stream samples show  
181 sudden change as the stream drops below the treeline.

## 182 **4. Discussion**

### 183 **4.1 Integration of local and upstream soil *n*-alkanes into the river sediments**

184 The hillslope soil leaf wax  $\delta\text{D}$ ,  $\delta^{13}\text{C}$  and ACL show a step-like change at the treeline,  
185 indicating a significant separation between upstream (above treeline) and downstream (below  
186 treeline) soils. Using this separation, it is possible to assess the contributions and integration of  
187 upstream vs. downstream soils to the streambed sediments along the altitude transect. The step-  
188 like transition in streambed  $\delta\text{D}$  and  $\delta^{13}\text{C}$  values indicates an over-printing of upstream alkane  
189 isotope values by input from deciduous vegetation. Thus, local production largely outweighs  
190 upstream transport in this setting. However, to firmly evaluate the upstream and downstream  
191 hillslope soil contribution to streambed sediments, there is a need to quantitatively evaluate the  
192 area-weighted production of *n*-alkanes above and below the treeline.

### 193 **4.2. Modeling *n*-alkane production and estimating upstream transport and integration**



194 To further evaluate the integration of *n*-alkanes above and below the treeline, we created a  
195 mixing model that calculates the expected  $\delta D$ ,  $\delta^{13}C$  and ACL values at each one of the sampling  
196 locations based on the *n*-alkane production of hillslope sediments above each streambed sampling  
197 point (Fig. 6). This mixing model assumes that the *n*-alkanes in the river are a function of the  
198 weighted *n*-alkane production above the sampling location.

199 The parameters we used for this mixing model are: 1. Satellite images to map the areas of  
200 tree and grass sediment throughout the Dany River catchment. 2. An estimate of net primary  
201 productivity of organic material production in grasses and trees (grams per area) (Brun et al.,  
202 2022). 3. Estimates of *n*-alkane production in grasses and trees in the Greater and Lesser Caucasus  
203 Mountains (grams of *n*-alkane per gram of organic material) (Trigui et al., 2019; Bliedtner et al.,  
204 2018). 4. End member values of  $\delta D$ ,  $\delta^{13}C$  and ACL derived from the average hillslope soils above  
205 and below the treeline. By multiplying these terms (area x organic mass production x *n*-alkane  
206 production x end member soils value), we created an *n*-alkane production map for the Dany River  
207 catchment. Using this map, we calculated, for each riverbed sampling location, the amount of grass  
208 and tree *n*-alkanes produced on the hillslopes above the sampling locations.

209 We compared the results of this mixing model with the measured  $\delta D$ ,  $\delta^{13}C$  and ACL in the  
210 streams. Stream sediment samples collected above the treeline (from ~2000-2600 masl) fall within  
211 the range of expected values, however, samples below the treeline consistently over-sample  
212 deciduous-sourced *n*-alkanes. Measured values do not have a linear relationship with the expected  
213 values based on vegetation area. These measured values would produce under-estimates of the  
214 upstream area of alpine grasses, yielding incorrect reconstructions of paleo-vegetation in  
215 sedimentary records. Comparing the mixing model with the observations indicates that an area-  
216 weighted mixing process is not an adequate model for explaining the *n*-alkanes signal in the



217 streambed sediments. A simple and straightforward way to interpret this discrepancy is that an  
218 area-weighted quantitative integration of *n*-alkanes is not a good model for describing this  
219 catchment system, and that local production is much larger than transported organic material.

220         However, there are still other factors that may be driving this process that our mixing model  
221 does not account for. First, the average slope of forested areas in the Dany watershed is higher than  
222 those in grassy areas. These steeper slopes would cause more sediment transport into the stream  
223 bed. Second, though production of *n*-alkanes in grasses and trees is not significantly different in  
224 the Greater and Lesser Caucasus Mountains, concentrations are higher in soils in deciduous areas  
225 (Trigui et al., 2019; Bliedtner et al., 2018). This retention of more biomarkers in forest soils would  
226 also increase the contribution of deciduous alkanes into the stream bed. Third, stream downcutting  
227 into older sediments has the potential to re-mobilize stored organic carbon, which may contain a  
228 greater load of deciduous *n*-alkanes. However, analysis of pollen from a nearby lake core in the  
229 Areguni Mountains shows a gradual shift over the last 4000 years from a grass-dominated  
230 landscape to the deciduous forest present today (Joannin et al., 2022). Therefore, stored biomarkers  
231 are more likely to be grass-dominant, and this is unlikely to explain the measured bias to deciduous  
232 alkanes.

233         Since *n*-alkanes in this first order stream do not quantitatively integrate *n*-alkanes based on  
234 the upstream area of different vegetation types, this likely precludes the use of *n*-alkanes as a tool  
235 to reconstruct vertical treeline movement in this setting. However, this is a benefit for attempts to  
236 reconstruct hydrological changes through the analysis of  $\delta D$  values in *n*-alkanes. Given the ~20%  
237 difference in apparent fractionation ( $\epsilon$ ) values for above and below treeline sediments, changes in  
238 upstream vegetation cover would alter measured  $\delta D$  values in *n*-alkanes in sedimentary archives.  
239 Without this quantitative integration, *n*-alkanes measured in the Pleistocene sediments found in



240 this watershed are more likely to reflect changes in  $\delta D$  values of precipitation, and therefore would  
241 serve to reconstruct hydrological cycles, rather than changes in upstream vegetation cover. Since  
242  $\delta^{13}C$  and ACL of *n*-alkanes are also different in above and below treeline sediments, these other  
243 analyses would also be useful to identify periods with large changes in treeline that might  
244 complicate interpretation of  $\delta D$  values.

245 In order to illustrate this point, we present hypothetical records of biomarker  $\delta D$  values  
246 from three points in the Dany watershed (Fig. 7) documenting 20‰ and 30‰ shifts in precipitation  
247  $\delta D$  values. Given the lack of quantitative integration in the catchment, a paleoclimate record from  
248 either above (A) or below (C) treeline would record the shift in precipitation  $\delta D$  values. Below  
249 treeline sedimentary records, with stream organic biomarker load overprinted by local vegetation  
250 production, would likely provide a means to reconstruct the  $\delta D$  precipitation values. However,  
251 records near the treeline (B) would be heavily affected by changes in apparent fractionation values  
252 associated with changes in vegetation around the stream. Co-occurring climate forcing of shifts in  
253  $\delta D$  values of precipitation and changes in treeline altitude would cause paleoclimate records in this  
254 zone to over-estimate the magnitude of precipitation  $\delta D$  value shifts.

255 Previous studies on the integration of organic biomarkers has produced mix results, with  
256 some demonstrating spatial integration of catchment signals (Alewell et al., 2016; Hemingway et  
257 al., 2016; Feakins et al., 2018b), whereas others did not observe this (Häggi et al., 2016b; Ponton  
258 et al., 2014). However, these previous studies typically focused on very large river systems, which  
259 will undergo different transport processes than the first-order streams analyzed in this study. A  
260 number of these studies (Alewell et al., 2016; Hemingway et al., 2016; Ponton et al., 2014; Feakins  
261 et al., 2018b) also observed seasonal differences in biomarker load in river sediments. Collecting



262 seasonal samples in the Areguni Mountains, as well as testing these processes in other first-order  
263 streams, could further help clarify the transport processes measured in this setting.

264

265

## 266 **5. Conclusion**

267 Sediment and stream samples from the Areguni Mountains, a subrange of the Lesser Caucasus  
268 Mountains in Armenia, demonstrate that there is a significant difference in hillslope soil  $\delta D$ ,  $\delta^{13}C$   
269 and ACL values above and below treeline. *n*-alkanes in sediments in the Areguni Mountains can  
270 be used to differentiate between the above and below treeline sediments. However, *n*-alkanes  
271 extracted from stream sediments reflect their local area, rather than demonstrating transport from  
272 the higher-altitude alpine meadow. These results provide a complication for attempts to reconstruct  
273 changes in past treeline in this mountain range, given that the biomarker load in stream does not  
274 reflect the relative area of different upstream vegetation types. However, these results simplify  
275 interpretation of past *n*-alkane  $\delta D$  values, as apparent fractionation differences between grasses  
276 and trees are less likely to impart a significant influence on  $\delta D$  values in stream bed *n*-alkanes.

## 277 **6. Competing interests**

278 The contact author has declared that none of the authors has any competing interests

## 279 **7. Acknowledgements**

280 We would like to thank the Kalavan villagers for their help, support, and hospitality: especially  
281 the Ghukasyan family for providing us a home away from home. We also thank Suren Kesejyan,  
282 Hovhannes Partevyan, and Vardan Stepanyan. The research in Kalavan project was funded by the  
283 support of The Gerda Henkel Stiftung grant n. AZ 10\_V\_17 and n. AZ 23/F/19, the Leakey  
284 Foundation. AB is thankful to the Lady Davis foundation, Fritz-Thyssen Foundation grant awarded



285 for the project “Pleistocene Hunter-Gatherer Lifeways and Population Dynamics in the Ararat  
286 (paleo-lake) Depression, Armenia”, and The European Research Council grant N 948015:  
287 “Investigating Pleistocene population dynamics in the Southern Caucasus” (awarded to AMB) for  
288 current financial support. Further support was provided by “Areni-1 Cave” Consortium [“Areni-1  
289 Cave” Scientific-Research Foundation (Armenia), and the "Gfoeller Renaissance Foundation”  
290 (USA)], as well as the Institute of Archaeology and Ethnography of the National Academy of  
291 Sciences of the Republic of Armenia (supported by the Higher Education and Science Committee,  
292 Republic of Armenia, under grant number 21AG-6A080).

293



294

## Works Cited

295

296 Alewell, C., Birkholz, A., Meusburger, K., Schindler Wildhaber, Y., and Mabit, L.: Quantitative  
297 sediment source attribution with compound-specific isotope analysis in a C3 plant-  
298 dominated catchment (central Switzerland), *Biogeosciences*, 13, 1587–1596,  
299 <https://doi.org/10.5194/bg-13-1587-2016>, 2016.

300 Antonelli, A., Kissling, W. D., Flantua, S. G. A., Bermúdez, M. A., Mulch, A., Muellner-Riehl,  
301 A. N., Kreft, H., Linder, H. P., Badgley, C., Fjeldså, J., Fritz, S. A., Rahbek, C., Herman,  
302 F., Hooghiemstra, H., and Hoorn, C.: Geological and climatic influences on mountain  
303 biodiversity, *Nat Geosci*, 11, 718–725, <https://doi.org/10.1038/s41561-018-0236-z>, 2018.

304 Bliedtner, M., Schäfer, I. K., Zech, R., and Von Suchodoletz, H.: Leaf wax n-alkanes in modern  
305 plants and topsoils from eastern Georgia (Caucasus) - Implications for reconstructing  
306 regional paleovegetation, *Biogeosciences*, 15, 3927–3936, <https://doi.org/10.5194/bg-15-3927-2018>, 2018.

308 Brun, P., Zimmermann, N. E., Hari, C., Pellissier, L., and Karger, D. N.: Global climate-related  
309 predictors at kilometer resolution for the past and future, *Earth Syst Sci Data*, 14, 5573–  
310 5603, <https://doi.org/10.5194/essd-14-5573-2022>, 2022.

311 Bush, R. T. and McInerney, F. A.: Leaf wax n-alkane distributions in and across modern plants:  
312 Implications for paleoecology and chemotaxonomy, *GeochimCosmochim Acta*, 117, 161–  
313 179, <https://doi.org/10.1016/j.gca.2013.04.016>, 2013.

314 Diefendorf, A. F. and Freimuth, E. J.: Extracting the most from terrestrial plant-derived n-alkyl  
315 lipids and their carbon isotopes from the sedimentary record: A review, *Org Geochem*,  
316 103, 1–21, <https://doi.org/10.1016/j.future.2015.08.005>, 2017.



- 317 Diefendorf, A. F., Freeman, K. H., Wing, S. L., and Graham, H. V.: Production of n-alkyl lipids  
318 in living plants and implications for the geologic past, *Geochim Cosmochim Acta*, 75,  
319 7472–7485, <https://doi.org/10.1016/j.gca.2011.09.028>, 2011.
- 320 Ehleringer, J., Björkman, O., and Bjorkman, O.: Quantum yields for CO<sub>2</sub> uptake in C<sub>3</sub> and C<sub>4</sub>  
321 plants, *Plant Physiol*, 59, 86–90, 1977.
- 322 Farquhar, G. D., O’Leary, M. H., and Berry, J. A.: On the Relationship between Carbon Isotope  
323 Discrimination and the Intercellular Carbon Dioxide Concentration in Leaves, *Aust J Plant*  
324 *Physiol*, 9, 121–137, 1982.
- 325 Feakins, S. J., Wu, M. S., Ponton, C., Galy, V., and West, A. J.: Dual isotope evidence for  
326 sedimentary integration of plant wax biomarkers across an Andes-Amazon elevation  
327 transect, *Geochim Cosmochim Acta*, 242, 64–81,  
328 <https://doi.org/10.1016/j.gca.2018.09.007>, 2018a.
- 329 Feakins, S. J., Wu, M. S., Ponton, C., Galy, V., and West, A. J.: Dual isotope evidence for  
330 sedimentary integration of plant wax biomarkers across an Andes-Amazon elevation  
331 transect, *Geochim Cosmochim Acta*, 242, 64–81,  
332 <https://doi.org/10.1016/j.gca.2018.09.007>, 2018b.
- 333 Ficken, K. J., Li, B., Swain, D. L., and Eglinton, G.: An n -alkane proxy for the sedimentary input  
334 of submerged floating freshwater aquatic macrophytes, *Org Geochem*, 31, 745–749, 2000.
- 335 Gasparyan, B., and Glauberman, P.: Beyond European boundaries: Neanderthals in the Armenian  
336 Highlands and the Caucasus. *Updating Neanderthals*. Academic Press, 275-301, 2022
- 337 Gamarra, B., Sachse, D., and Kahmen, A.: Effects of leaf water evaporative 2H-enrichment and  
338 biosynthetic fractionation on leaf wax n-alkane  $\delta^2\text{H}$  values in C<sub>3</sub> and C<sub>4</sub> grasses, *Plant*  
339 *Cell Environ*, 39, 2390–2403, <https://doi.org/10.1111/pce.12789>, 2016.



- 340 Ghukasyan, R., Colonge, D., Nahapetyan, S., Ollivier, V., Gasparyan, B., Monchot, H., and  
341 Chataigner, C.: Kalavan-2 (North of Lake Sevan, Armenia): A new late middle paleolithic  
342 site in the Lesser Caucasus, *Archaeology, Ethnology and Anthropology of Eurasia*, 38, 39–  
343 51, <https://doi.org/10.1016/j.aeae.2011.02.003>, 2010.
- 344 Guisan, A. and Theurillat, J.-P.: Assessing alpine plant vulnerability to climate change: a modeling  
345 perspective., *Integrated Assessment*, 307–320, 2000.
- 346 Häggi, C., Sawakuchi, A. O., Chiessi, C. M., Mulitza, S., Mollenhauer, G., Sawakuchi, H. O.,  
347 Baker, P. A., Zabel, M., and Schefuß, E.: Origin, transport and deposition of leaf-wax  
348 biomarkers in the Amazon Basin and the adjacent Atlantic, *GeochimCosmochim Acta*,  
349 192, 149–165, <https://doi.org/10.1016/j.gca.2016.07.002>, 2016a.
- 350 Häggi, C., Sawakuchi, A. O., Chiessi, C. M., Mulitza, S., Mollenhauer, G., Sawakuchi, H. O.,  
351 Baker, P. A., Zabel, M., and Schefuß, E.: Origin, transport and deposition of leaf-wax  
352 biomarkers in the Amazon Basin and the adjacent Atlantic, *GeochimCosmochim Acta*,  
353 192, 149–165, <https://doi.org/10.1016/j.gca.2016.07.002>, 2016b.
- 354 Hemingway, J. D., Schefuß, E., Dinga, B. J., Pryer, H., and Galy, V. V.: Multiple plant-wax  
355 compounds record differential sources and ecosystem structure in large river catchments,  
356 *GeochimCosmochim Acta*, 184, 20–40, <https://doi.org/10.1016/j.gca.2016.04.003>, 2016.
- 357 Jetter, R., Kunst, L., and Samuels, A. L.: Composition of plant cuticular waxes, in: *Biology of the*  
358 *Plant Cuticle*, edited by: Riederer, M. and Miller, C., Blackwell Publishing Ltd, Oxford,  
359 145–181, 2006.
- 360 Joannin, S., Capit, A., Ollivier, V., Bellier, O., Brossier, B., Mourier, B., Tozalakian, P., Colombié,  
361 C., Yevadian, M., Karakhanyan, A., Gasparyan, B., Malinsky-Buller, A., Chataigner, C.,  
362 and Perello, B.: First pollen record from the Late Holocene forest environment in the Lesser



- 363           Caucasus, *Rev PalaeobotPalynol*, 304, <https://doi.org/10.1016/j.revpalbo.2022.104713>,  
364           2022.
- 365   Malinsky-Buller, A., Glauberman, P., Ollivier, V., Lauer, T., Timms, R., Frahm, E., Brittingham,  
366           A., Triller, B., Kindler, L., Knul, M. V., Krakovsky, M., Joannin, S., Hren, M. T., Bellier,  
367           O., Clark, A. A., Blockley, S. P. E., Arakelyan, D., Marreiros, J., Paixaco, E., Calandra, I.,  
368           Ghukasyan, R., Nora, D., Nir, N., Adigyoalyan, A., Haydosyan, H., and Gasparyan, B.:  
369           Short-Term occupations at high elevation during the Middle Paleolithic at Kalavan 2  
370           (Republic of Armenia), *PLoS One*, 16, <https://doi.org/10.1371/journal.pone.0245700>,  
371           2021.
- 372   Montoya, C., Balasescu, A., Joannin, S., Ollivier, V., Liagre, J., Nahapetyan, S., Ghukasyan, R.,  
373           Colonge, D., Gasparyan, B., and Chataigner, C.: The Upper Palaeolithic site of Kalavan 1  
374           (Armenia): An Epigravettian settlement in the Lesser Caucasus, *J Hum Evol*, 65, 621–640,  
375           <https://doi.org/10.1016/j.jhevol.2013.07.011>, 2013.
- 376   Oakes, A. M. and Hren, M. T.: Temporal variations in the  $\delta D$  of leaf n-alkanes from four riparian  
377           plant           species,           *Org           Geochem*,           97,           122–130,  
378           <https://doi.org/10.1016/j.orggeochem.2016.03.010>, 2016.
- 379   Pedentchouk, N., Sumner, W., Tipple, B., and Pagani, M.:  $\delta^{13}C$  and  $\delta D$  compositions of n-alkanes  
380           from modern angiosperms and conifers: An experimental set up in central Washington  
381           State,           USA,           *Org           Geochem*,           39,           1066–1071,  
382           <https://doi.org/10.1016/j.orggeochem.2008.02.005>, 2008.
- 383   Ponton, C., West, A. J., Feakins, S. J., and Galy, V.: Leaf wax biomarkers in transit record river  
384           catchment           composition,           *Geophys           Res           Lett*,           41,           6420–6427,  
385           <https://doi.org/10.1002/2014GL061184>.Received, 2014.



- 386 Sachse, D., Billault, I., Bowen, G. J., Chikaraishi, Y., Dawson, T. E., Feakins, S. J., Freeman, K.  
387 H., Magill, C. R., McInerney, F. a., van der Meer, M. T. J. J., Polissar, P., Robins, R. J.,  
388 Sachs, J. P., Schmidt, H.-L., Sessions, A. L., White, J. W. C., West, J. B., and Kahmen, A.:  
389 Molecular paleohydrology: interpreting the hydrogen-isotopic composition of lipid  
390 biomarkers from photosynthesizing organisms, *Annu Rev Earth Planet Sci*, 40, 221–249,  
391 <https://doi.org/10.1146/annurev-earth-042711-105535>, 2012.
- 392 Sikes, E. L., Medeiros, P. M., Augustinus, P., Wilmshurst, J. M., and Freeman, K. R.: Seasonal  
393 variations in aridity and temperature characterize changing climate during the last  
394 deglaciation in New Zealand, *Quat Sci Rev*, 74, 245–256,  
395 <https://doi.org/10.1016/j.quascirev.2013.01.031>, 2013.
- 396 Suh, Y. J., Diefendorf, A. F., Bowen, G. J., Cotton, J. M., and Ju, S. J.: Plant wax integration and  
397 transport from the Mississippi River Basin to the Gulf of Mexico inferred from GIS-  
398 enabled isoscapes and mixing models, *GeochimCosmochim Acta*, 257, 131–149,  
399 <https://doi.org/10.1016/j.gca.2019.04.022>, 2019.
- 400 Tornero, C., Balasse, M., Bălăşescu, A., Chataigner, C., Gasparyan, B., and Montoya, C.: The  
401 altitudinal mobility of wild sheep at the Epigravettian site of Kalavan 1 (Lesser Caucasus,  
402 Armenia): Evidence from a sequential isotopic analysis in tooth enamel, *J Hum Evol*, 97,  
403 27–36, <https://doi.org/10.1016/j.jhevol.2016.05.001>, 2016.
- 404 Trigui, Y., Wolf, D., Sahakyan, L., Hovakimyan, H., Sahakyan, K., Zech, R., Fuchs, M., Wolpert,  
405 T., Zech, M., and Faust, D.: First calibration and application of leaf wax n-alkane  
406 biomarkers in loess-paleosol sequences and modern plants and soils in Armenia,  
407 *Geosciences (Switzerland)*, 9, <https://doi.org/10.3390/geosciences9060263>, 2019.
- 408 Zazanashvili, N.: *The Caucasus Hotspot*, 2009.



420 Figure Captions

421 Figure 1: (Left) Topographic map of Armenia with inset map of sampling location (black box)  
422 (Right) Inset map of soil (yellow circles) and stream (blue circles) samples collected in the  
423 Areguni Mountains, along with the limit of the Barepat (dashed line) and Dany watersheds (solid  
424 line)

425 Figure 2: The  $\delta D$  and  $\delta^{13}C$  values of *n*-alkanes extracted from above treeline (green squares) and  
426 below treeline (red triangles) sediments

427 Figure 3: The average chain length (ACL) values of *n*-alkanes extracted from above treeline  
428 (green squares) and below treeline (red squares) and stream (blue triangles) sediments across the  
429 sampling elevation gradient

430 Figure 4: The  $\delta^{13}C$  values of *n*-alkanes extracted from above treeline (green squares) and below  
431 treeline (red squares) and stream (blue triangles) sediments across the sampling elevation  
432 gradient

433 Figure 5: The  $\delta D$  values of *n*-alkanes extracted from above treeline (green squares) and below  
434 treeline (red squares) and stream (blue triangles) sediments across the sampling elevation  
435 gradient

436 Figure 6: Comparison of the measured ACL,  $\delta D$  and  $\delta^{13}C$  values against expected values of  
437 stream sediments. Dashed line represents the range of expected values from stream sediments if  
438 vegetation was integrated equally by area

439 Figure 7: A photograph of the Dany watershed with hypothetical paleoclimate record from three  
440 locations: (A, dashed line) Below treeline, (B, solid line) near treeline with fluctuations in  
441 treeline altitude, and (C, dotted line) above treeline

442

443



444

445

446

447

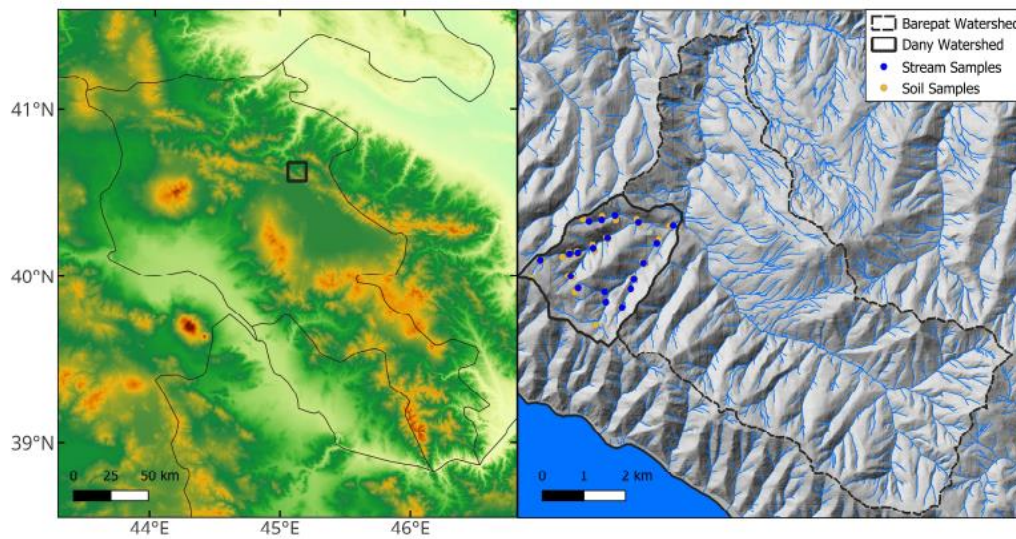


Figure 1: (Left) Topographic map of Armenia with inset map of sampling location (black box) (Right) Inset map of soil (yellow circles) and stream (blue circles) samples collected in the Areguni Mountains, along with the limit of the Barepat (dashed line) and Dany watersheds (solid line)



448

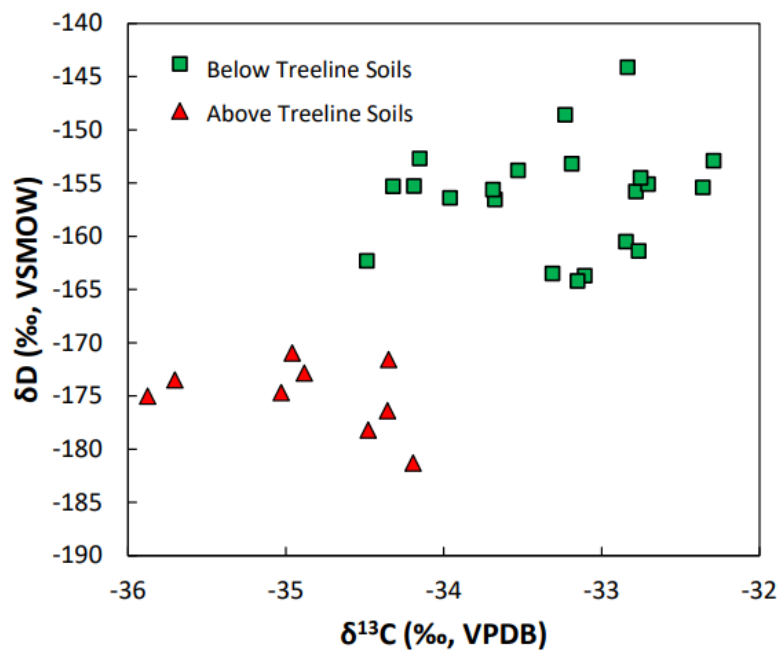


Figure 2: The  $\delta\text{D}$  and  $\delta^{13}\text{C}$  values of *n*-alkanes extracted from above treeline (green squares) and below treeline (red triangles) sediments



449

450

451

452

453

454

455

456

457

458

459

460

461

462

463

464

465

466

467

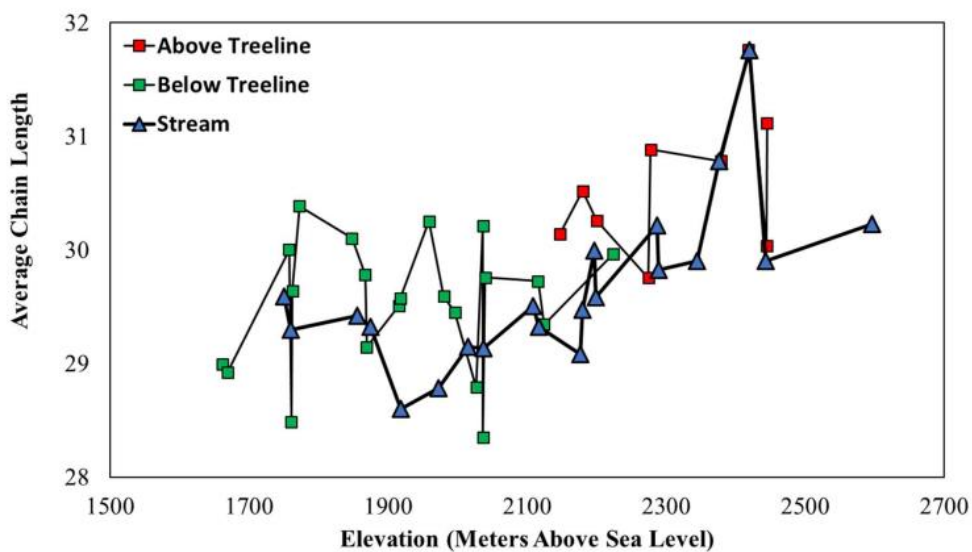


Figure 3: The average chain length (ACL) values of *n*-alkanes extracted from above treeline (green squares) and below treeline (red squares) and stream (blue triangles) sediments across the sampling elevation gradient



468

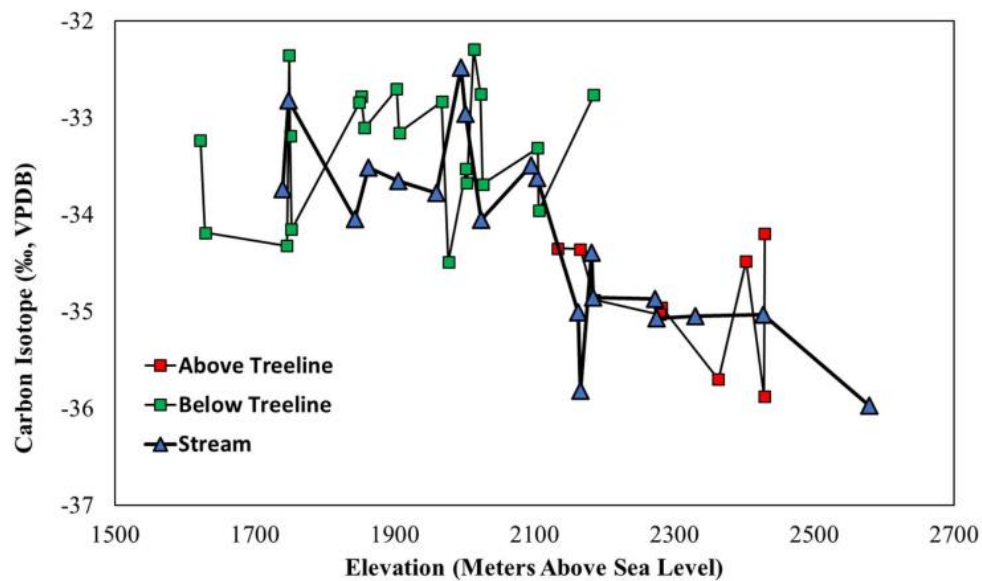


Figure 4: The  $\delta^{13}C$  values of *n*-alkanes extracted from above treeline (green squares) and below treeline (red squares) and stream (blue triangles) sediments across the sampling elevation gradient



469  
470  
471  
472  
473  
474  
475  
476  
477  
478  
479  
480  
481  
482  
483  
484  
485  
486  
487

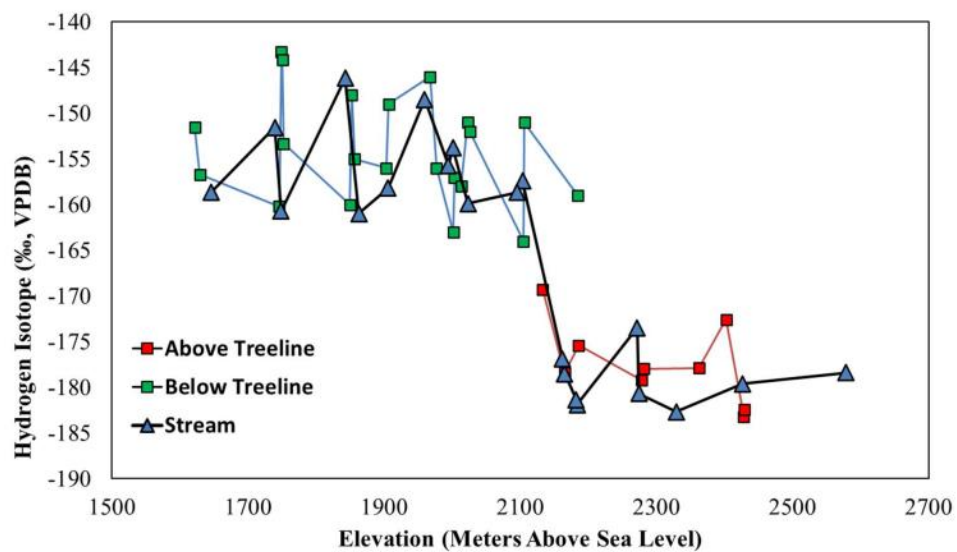


Figure 5: The  $\delta D$  values of *n*-alkanes extracted from above treeline (green squares) and below treeline (red squares) and stream (blue triangles) sediments across the sampling elevation gradient



488

489

490

491

492

493

494

495

496

497

498

499

500

501

502

503

504

505

506

507

508

509

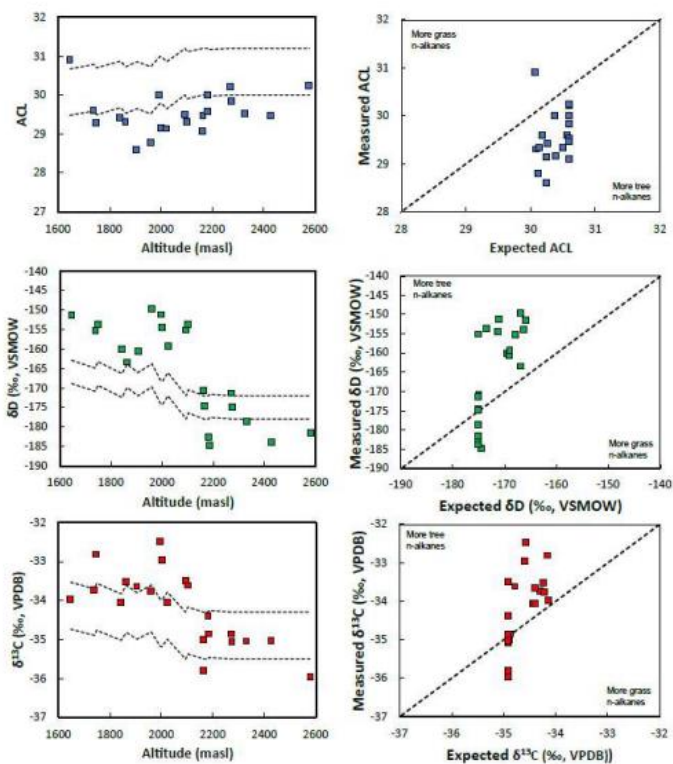


Figure 6: Comparison of the measured ACL,  $\delta D$  and  $\delta^{13}C$  values against expected values of stream sediments. Dashed line represents the range of expected values from stream sediments if vegetation was integrated equally by area



510

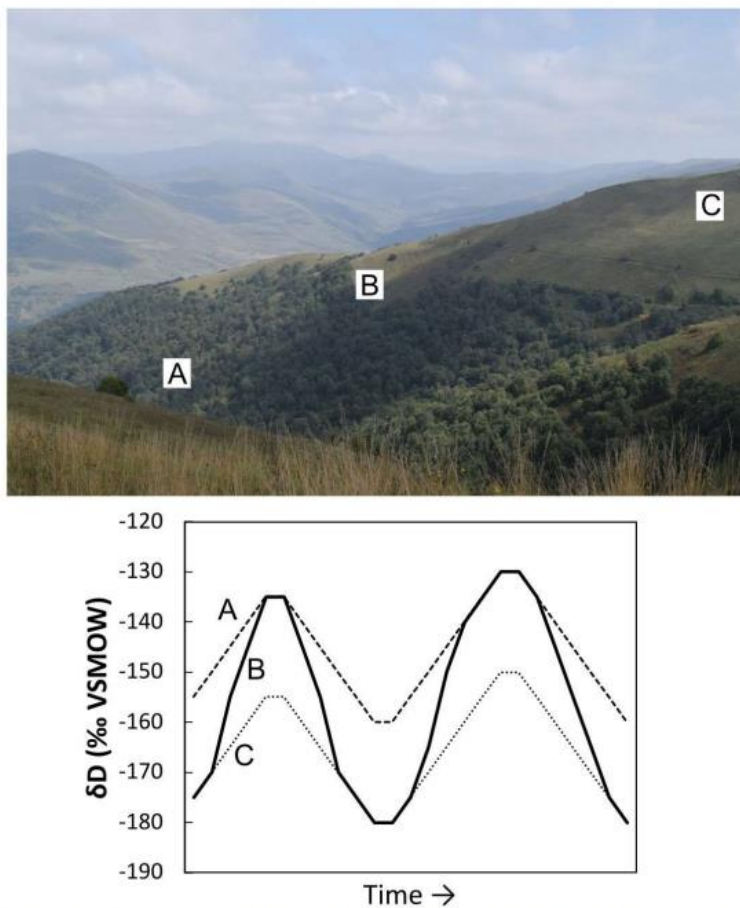


Figure 7: A photograph of the Dany watershed with hypothetical paleoclimate record from three locations: (A, dashed line) Below treeline, (B, solid line) near treeline with fluctuations in treeline altitude, and (C, dotted line) above treeline